

Correlation Characteristics between Vertically and Horizontally Polarized Components of Arriving Radio Wave during Shadowing by Human Body

#Tokio Taga¹, Tetsuro Imai²

¹Graduate School of Science & Technology, Kwansai Gakuin University
2-1 Gakuen Sanda, Japan, taga@kwansai.ac.jp

²Radio Access Network Development Department, NTT DoCoMo, Inc.
3-5 Hikari-no-oka Yokosuka, Japan, imait@nttdocomo.co.jp

1. Introduction

No correlation between vertically and horizontally polarized radio wave has been assumed in most land mobile communication environments [1]. In a line-of-sight (LOS) radio propagation environment such as an indoor radio LAN, both base and mobile terminals are operated at rest, and the propagation paths comprise multiple paths with different polarization ratios. When a human body moves around the terminals, the main polarized and cross polarized components incur the influence of the shadowing simultaneously. Thus, it is to be expected that these polarized components have a correlation. It is also expected that the polarization correlation affects the performance of polarized MIMO antenna systems, but there is no literature in which its formulations and effects are described.

This paper presents calculation results for the polarization correlation when a human body shadows a propagation path and measured results using a high-resolution channel sounder in a 5.2GHz band.

2. Computer Simulation

2.1 Human body model

Fig. 1 shows the human body model used in this study. A dielectric rectangular model with finite height is assumed as the human body model. Its height is assumed to be 172 cm, which is the average height of Japanese male, and its thickness and width are assumed to be 20 cm and 35 cm, respectively. The electrical material constants of the human parts are presented in [2], and the permittivity and conductivity of the human muscle are used in this calculation. The permittivity and conductivity of the human muscle is $\epsilon_r = 49.54$ and $\sigma = 4.0448$ [S/m] in a 5 GHz band, respectively.

2.2 Calculation model for path shadowing

Fig. 2 shows a calculation model for shadowing a direct path using the human body model. A movement route for the human model is a straight line that intersects the direct path between the transmitting point and receiving point, and has a crossing angle of θ . The distance between the transmitting and receiving points is L_d [m], the distance from the transmitting point to the center point of the rectangular human model when it crosses the direct path line is L [m], and the distance that the human model moves along the movement route is L_m [m]. The range of L_m is defined from -1.4 m to 1.4 m, and the local origin of L_m is set at the cross point of the direct path. By setting this range, a single diffracted path (S2) described as follows exists in all the calculations. The calculation condition and parameters are given in Table 1. In this paper, θ is assumed to be 45 [deg]. As shown in Fig. 3, it is assumed that seven paths, one direct path, two single diffracted paths, and four double diffracted paths, mainly contribute to the received field strength. Since this study considers the effect of variation between the cross-polarized components including the direct path, so the ground reflected path and the other paths propagating over/through the human model are not taken into account. According to the measured results in [3], paths passing over the head of the human model are also disregarded. The propagation routes of six diffracted paths, two single diffracted paths and four double diffracted paths, are shown in Fig. 3. When the human body shadows the direct path, the paths diffracted at the edges of the rectangular block arrive at the receiving point. The heuristic Uniform Theory of Diffraction (UTD) formulas for dielectric materials are adopted for estimating the received field strength in this calculation. The heuristic

UTD formula presented by El-Sallabi [4] is used for single diffraction, and that by Luebbers [5] is used for double diffraction.

2.3 Calculation results of received field strength

Fig. 4 shows characteristics of the received field strength for the distance that the human model moved. Figs. 4(a) and 4(b) show the results for $L = 3$ m and $L_d/2$ [m] in a case of $L_d = 30$ m, respectively. A variation is observed between the V and H polarization components for the entire moving distance, but there is no marked difference in the distance range from -0.28 m to 0.28 m, which is the interval that the human model shadowed the direct path geometrically, and is called the "human shadowing region" in this paper. When L is $L_d/2$, the longer L is, the smaller the difference in the received field strength is obtained. This tendency for a smaller difference in the human shadowing region becomes remarkable when the path length is longer and distance L is longer. We can easily expected that the correlation between cross polarization components will become closer to one.

The characteristics outside this human shadowing region vary and comprise the direct path and the other diffracted paths from the human model. So in this region, the direct path field and the field comprising diffracted paths should be treated as two distinguished paths. Thus, in this paper, the calculated data are divided into three parts as shown in Fig. 5, which are the human shadowing region and the other two regions neighboring it. In the following correlation analysis, the diffracted field strength data shown in Fig. 5(b) are treated as a path arriving from the human body.

2.4 Correlation between cross polarization

In this section, the distance of "human shadowing region (HSR)," from $L_m = -0.28$ m to 0.28 m, is assumed as the unit distance, and four more distance regions around the HSR are treated as non-shadowing regions. The correlation is expressed as ρ_{shad} for HSR, $\rho_{\text{us-1}}$ and $\rho_{\text{us+1}}$ for the adjoining regions of HSR, and $\rho_{\text{us-2}}$ and $\rho_{\text{us+2}}$ for the first and final regions on the route, respectively.

The field strengths are calculated every 2 mm on the route the human model moves, and 281 sampled data points are calculated and processed to obtain the correlation between the cross polarizations. Fig. 6 shows the calculated results for $L_d = 30$ m. In this figure, the abscissa indicates distance L from the transmitting point to the cross point between the direct path and the moving route. The top and bottom figures show correlation characteristics outside the HSR, and the middle figure shows that inside the HSR. This figure shows that the correlation is greater than 0.88 when L is greater than 3 m and that the correlation approaches one when L approaches to a half length of L_d . It is confirmed that the correlation is greater than 0.77 in cases of $L_d = 60$ m and 120 m. From these results, we expect that there is high correlation between the V and H polarization components.

3. Experiments

3.1 Measurement configuration

To investigate the time variation characteristics of the propagation path, a 5.2 GHz band channel sounder, RUSK-DoCoMo, was used and an indoor experiment was conducted. The measurement specifications are shown in Table 2. The measurements were carried out in a 6.7 m (W) x 9.6 m (D) x 2.8 m (H) room with no furniture. The distance between the transmitting and receiving antennas was 5.6 m. A vertically polarized half wavelength dipole antenna was used for the transmitter antenna. A cylindrical patch antenna array with 4x24 elements that has 2 ports for V and H polarization components, respectively, was used for the receiver antenna. The height of these antennas was set to 1.5 m. Three people walked along the routes at the velocity of 2 m/s during the measurements, and the human shadowing was recorded in the observed paths. The measured data are processed in resolution path numbers of 30 for the RIMAX algorithm [6].

3.2 Time variation characteristics and polarization correlation

Fourteen individual paths were resolved in this measurement. The path data for each path that had the same direction of arrival were extracted. Fig. 7 shows the path variation in the direction of $(\theta, \phi) = (91.5, 1.5)$ in degrees. This direction corresponds to that for the direct path from the transmitter antenna. We found that there are some missing data points in the time variation characteristics for both V and H path weight due to the resolution performance of the RIMAX algorithm. However, all the data were used to evaluate the correlation, and the results are shown in Fig. 8. We found that the polarization correlation is distributed in the range of 0.72 to 0.91 and has the mean of 0.85. Considering that the minimum path length between the antennas and human body is 1m practically in the measurement, the correlation may frequently be less than 0.7 or 0.8.

4. Conclusions

The correlation between the vertically and horizontally polarized components of the propagation path was investigated numerically and experimentally. The calculation results show that the polarization correlation is greater than 0.77 for the path length from 15 m to 120 m, and approaches one for the distances between the antennas and the human body of greater than 10 m. The measured results also show that the correlation is distributed in a range from approximately 0.7 to 0.9, and has the mean of 0.85. We conclude that the polarization has a high correlation.

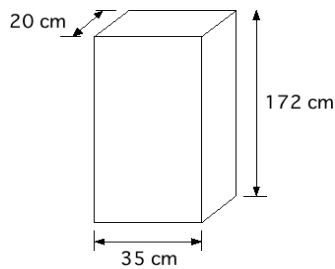


Figure 1: Dielectric rectangular human body model.

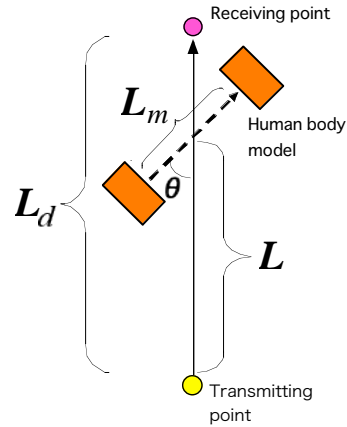


Figure 2: Calculation model for path shadowing.

Table 1: Calculation conditions and parameters.

Frequency	5 GHz
Directivity of transmitter (Tx) and receiver (Rx) antennas	Isotropic antenna($G=1$)
Height of Tx and Rx antennas	1.2 m
Distance between T and R points (L_d)	15, 30, 60, 120 m
Length from T to cross point of movement route and path (L)	Discretely selected in range of 3 to 60 m
Moving distance of human body model (L_m)	-1.4 to 1.4 m
Crossing angle θ	45 deg

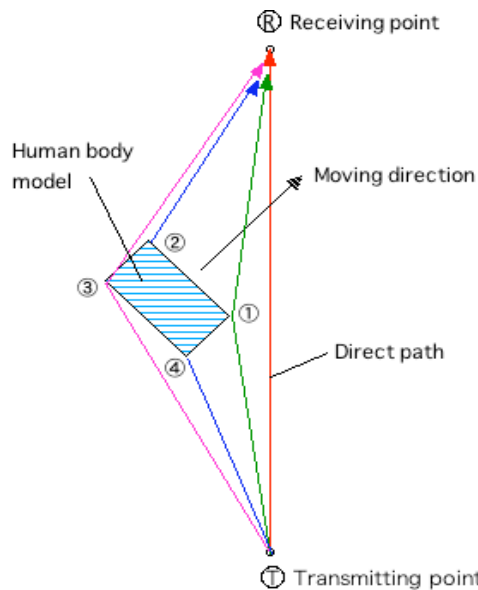


Figure 3: Propagation path route considered in this calculation.

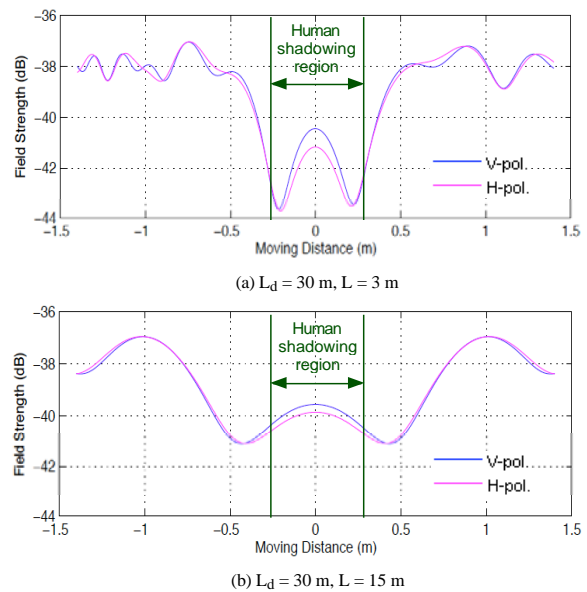


Figure 4: Characteristics of received field strength under shadowing in a case of $L_d = 15$ m.

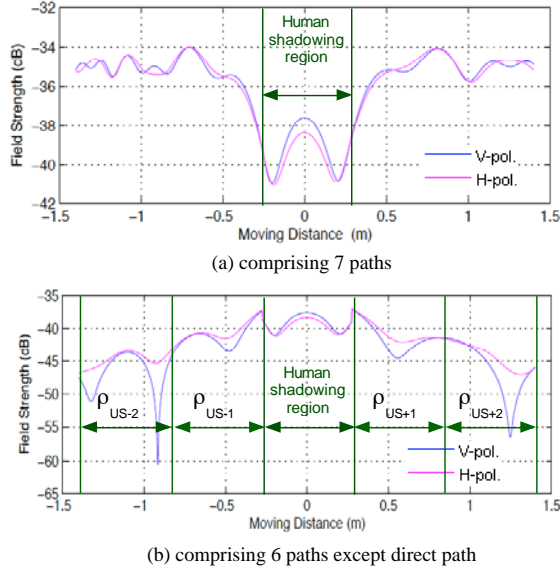


Figure 5: Field strength variation and sections for evaluating correlation between cross polarizations.

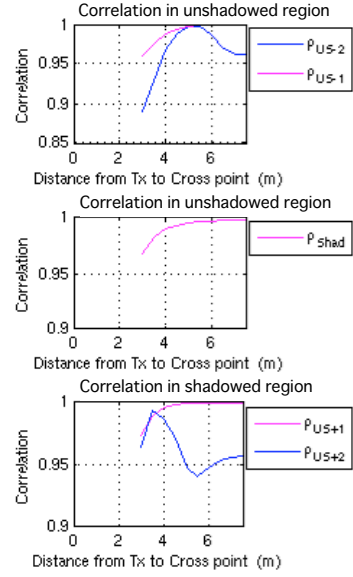


Figure 6: Calculated correlation characteristics between vertically and horizontally polarized components ($L_d = 30$ m).

Table 1: Measurement specifications.

Frequency	5.2 GHz	Sampling frequency	~ 39 Hz
Bandwidth	100 MHz	Measurement mode	Time Grid
Maximum time delay	0.8 msec		

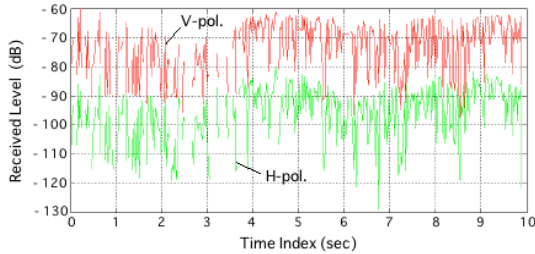


Figure 7: Measured time variation characteristics of a path arriving from $(\theta, \phi) = (91.5, 1.5)$ [deg] in V-pol. transmission.

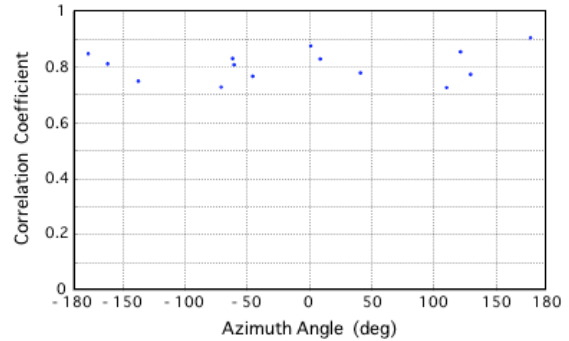


Figure 8: Distribution of measured correlation coefficients between vertically and horizontally polarized components in V-pol. transmission.

References

- [1] W. C. Jakes, Jr., *Microwave Mobile Communications*, New York: Wiley, Chap. 3, 1974.
- [2] <http://niremf.ifac.cnr.it/tissprop/>
- [3] T. Tsuji, T. Taga, T. Imai, "A study on calculation error of path shadowing due to human body using scattering pattern," Proceedings of the 2007 IEICE General Conference, B-1-32, 2007.
- [4] H. M. El-Sallabi, "A new heuristic diffraction coefficient for dielectric wedges at normal incidence," *IEEE Antennas Wireless Propagat. Lett.*, vol. 1, pp. 165- 168, 2002.
- [5] R. J. Luebbers, "A heuristic UTD slope diffraction coefficient for rough lossy wedges," *IEEE Transactions on Antennas and Propagation*, vol. 37, no. 2, pp. 206-211, Feb. 1989.
- [6] A. Richter, *Estimation of Radio Channel Parameters: Models and Algorithms*, Verlag ISLE, 2005.